CT Textural Analysis (CTTA) of Metastatic Treatment-Resistant Pancreatic Adenocarcinoma (PDAC): Identifying Biomarkers for Genetic Instability and Overall Survival

A thesis submitted to the University of Arizona College of Medicine – Phoenix
in partial fulfillment of the requirements for the degree of Doctor of Medicine

David Campbell
Class of 2016

Mentor: Ronald Korn, MD, PhD

Abstract

Significance: Metastatic, treatment-resistant pancreatic ductal adenocarcinoma (PDAC) is a rapidly fatal disease that typically carries a bleak prognosis. Contrast-enhanced CT is the current standard of care tool for imaging evaluation, and repeat imaging is routinely performed in clinical trials. The availability of these imaging data render them exploitable for further analysis. CT texural analysis (CTTA), a quantitative tool for examining a region of interest on CT and generating statistical parameters based on gray-level pixel data, is powerful technique that has been studied in other cancers and shown to correlate with features such as tumor grade, stage, and prognosis. However, the application of CTTA to PDAC has not been studied. Given the paucity of diagnostic tests to guide therapy, validated CTTA biomarkers could be immensely useful. Identifying PDAC variants that have a relative deficit in DNA repair might allow these cancers to be treated with targeted cytotoxic regimens sooner. Additionally, identifying prognostic CTTA parameters would be useful in gauging the severity of disease.

Objective: We sought to perform quantitative textural analysis on CT imaging from a clinical trial cohort of patients with metastatic, treatment-resistant PDAC. We aimed to correlate CTTA features to molecular profiling results (copy number variations obtained by array CGH) and clinical features (overall survival).

Design: Metastatic tumor sites from patients with treatment-resistant PDAC were biopsied and molecularly profiled. Intrachromosal copy number were assessed by CGH in tumor specimens, and patients were treated based on these individual molecular profiling results. Pre-biopsy portal-venous phase and non-contrast CT scans were obtained for retrospective analysis (n=15). CTTA was performed by drawing regions of interest around the primary pancreas adenocarcinoma and the normal pancreas tissue. CTTA parameters including mean positive pixels, entropy, kurtosis, and skewness were derived using the TexRAD platform at texture filtering densities of 0, 2, 3, 4, 5, and 6 pixels. CTTA values were then compared to intrachromosomal copy number variation (CNV) per tumor and overall survival (OS) post-

treatment using a Spearman's rank correlation coefficient. Additional linear regression analysis was performed for positive correlations, and a Kaplan-Meier statistic was generated for OS using median CTTA entropy. Multivariate analyses for CNV and OS were also performed.

Results: CNV were negatively correlated with the kurtosis value of the primary tumor mass using medium texture filtering ($p=0.034$, $n=15$). Linear regression revealed a significant negative correlation between kurtosis and CNV ($p=0.038$). Secondary analysis of the normal pancreas using coarse texture filtering revealed that increasing entropy was associated with decreased OS ($p=0.0014$, $n=12$). Using median entropy as a cutoff value (median: 4.165), median OS was greater in the entropy < 4.165 group versus the entropy > 4.165 group (179 days v 43 days; 95% CI 73.137 – 166.87; $p=0.004$, $n=12$).

Conclusions: This exploratory study with admittedly limited sample size raises interesting questions about the use of CTTA parameters as diagnostic tools and/or biopsy adjuncts in assessing PDAC susceptibility to commercially available cytotoxics. Secondarily, entropy, a potential marker of heterogeneity and inflammation in the normal pancreas, represents an intriguing possibility for gauging prognosis.

Table of Contents:

Figures and Tables:

Introduction

Pancreatic ductal adenocarcinoma (PDAC) is an insidious and rapidly fatal malignancy. Given the current lack of effective screening methods and often nonspecific clinical signs, metastatic disease is the initial presentation in about half of new cases[1]. In the last several decades, the improved prevention, detection, and treatment of more common cancers have lessened their burden. However, similar efforts to combat PDAC have been met with modest gains, and as a result it has become the fourth leading cause of cancer death in the US[2]. Effective chemotherapeutic options are limited, resistance develops swiftly, and there is a lack of suitable tests to guide treatment. Ensuring application of the most effective combination of chemotherapeutics therefore presents a formidable challenge. Characterizing each patient's individual cancer by its molecular and genetic characteristics is one option for pursuing more efficacious, personalized therapy. If successful, biopsy with molecular profiling would become a fundamental step in the management of treatment-resistant PDAC. Current efforts include the identification and treatment of a subset of pancreatic cancer characterized by frequent double stranded DNA breaks, signifying a defect in homologous end-joining DNA repair as seen in BRCA 1 / 2 mutations. These cancers may be more susceptible to cytotoxic regimens and poly(ADP-ribose) polymerase inhibitors (PARP-i). Clinical trials are currently underway to demonstrate or dismiss the efficacy of such regimens[3].

One challenging aspect of molecular profiling is that pancreatic cancer continues to evolve over time and in response to treatment. As powerful a tool as it may be, a biopsy is a static representation unless it is repeated. Serial biopsies are costly, impractical, and not without risk and inconvenience to the patient. As it stands, the availability of additional diagnostic tests to characterize and typify pancreatic cancer to guide treatment is an unmet need. A possible solution is exploiting imaging data that already exists. Standard-of-care CT imaging for response assessment is routinely acquired on a regular basis. CT Textural Analysis (CTTA), a method for extracting detailed statistical information from imaging sets, is a promising and emerging clinical decision support tool to further characterize cancer morphology without the need for other imaging modalities (i.e. PET, MRI) or additional procedures. The analysis of these data yields descriptive statistical parameters such as kurtosis, entropy, and skewness

derived from a histogram of the gray-level pixel intensities in an operator-selected region of interest. These CTTA parameters have been shown to correlate with relevant histopathologic features such as tumor vascularity, grade, stage, gene amplification, and differentiating malignant versus benign lesions in a number of cancers[4-10]. Additionally, relevant clinical endpoints like overall survival and treatment response have been shown to correlate with CTTA features[11-17]. Though it could never replace conventional diagnostic procedures, the secondary CTTA analysis of routinely acquired imaging could be used as a "virtual biopsy" to gain more actionable information on a patient's cancer. If validated, CTTA parameters could function as biomarkers to help guide treatment decisions. However, CTTA of PDAC has not been studied, so the utility of such an approach is currently unknown.

In this study, we sought to explore the CTTA features of a unique subset of stage IV treatment-resistant pancreatic cancers found to exhibit a large number of copy number variations (CNV) by Comparative Genomic Hybridization (CGH). Recent studies have shown that increased copy number variations (CNV) in PDAC specimens coincides with an unstable genome and constitutive inactivation of DNA maintenance genes (BRCA1, BRCA2, and PALB2)[18]. Additionally, this cancer subtype responds better to platinum-based cytotoxic therapy[19]. We hypothesized that CTTA parameters such as kurtosis and entropy, which have been shown to correlate with genomic features and prognosis in other cancers, might also correlate with differentiating features of this genomic variant. Secondary analysis of CTTA parameters in relation to overall survival was also performed.

Materials and Methods

Patients in clinical trial

IRB ethical approval was obtained for analysis of previously acquired CT imaging data from a molecular profiling-based Phase II clinical trial conducted through the Virginia G. Piper Cancer Center in Scottsdale, AZ (ClinicalTrials.gov identifier: NCT01196247 / SU2C-001). The trial, conducted from September 2010 to February 2012, examined the effectiveness of molecular-profiling guided chemotherapy on advanced, treatment-resistant metastatic pancreatic cancer. Financial support was provided by a grant from the SU2C/AACR-pancreatic dream team. Inclusion criteria encompassed age greater than 18, at least one prior therapy, adequate organ and bone marrow function, Karnofsky performance score greater than 70, one or more metastatic tumors measurable by CT, and at least one metastasis amenable to biopsy. Exclusion criteria were operable or locally advanced PDAC, known brain metastasis (unless previously treated and well controlled), active or uncontrolled infection, known HIV/HBV/HCV infection, and pregnant or breast-feeding patients. 47 patients were enrolled into the trial. 10 patients were screening failures and 2 did not receive treatment and were therefore excluded. The remaining 35 patients underwent a tumor biopsy of a metastatic site (typically liver). 85% of the cohort had 1-3 previous treatment regimens, and the remaining 15% had 4-6.

Biopsy and molecular profiling

Pre-biopsy triple phase abdominal CT scans were performed for staging no more than two weeks prior to tumor sampling. Biopsy samples were sent for immunohistochemistry (IHC), microarray-based comparative genomic hybridization (array CGH), and gene expression microarray. IHC and array CGH were performed at the Translational Genomics Research Institute in Scottsdale, AZ. Gene expression microarray was completed at John Hopkins University[20].

CGH is a technique to detect unbalanced chromosomal alterations. Tumor DNA is denatured into single strands, labelled with green fluorochromes, and mixed in equal concentration with a control sample of normal DNA labeled with red fluorochromes. These samples are added to preparations of cDNA. Each sample competes equally for hybridization to their loci of origin. Array CGH, used in this trial, is an improvement upon traditional CGH with improved sensitivity

for detecting smaller aberrations[21]. The comparison along the axis of each chromosome permits the detection of chromosomal amplifications and deletions recorded as copy number variations (CNV) by measuring the differential fluorescence ratio[22]. Diploid and aneuploid tumor cell populations from biopsy samples were flow sorted, processed, and hybridized to 400,000 feature CGH arrays. The combined use of IHC and CGH were used to interrogate a variety of therapeutic targets. Patients were then treated with commercially available cytotoxic regimens based on these individual molecular profiling results. Overall survival and treatment response from the start of clinical trial therapy were recorded for each patient[20].

Patients selected for CTTA study

CT imaging available in the PACS database varied for each patient who completed the clinical trial. There were a combination of non-contrast and contrast-enhanced arterial, portal venous, hepatic, and delayed phase imaging. The portal venous phase and non-contrast scans were selected for analysis due to their obtainability (n = 17). The remaining 18 patients did not have portal-venous phase or non-contrast CT imaging available for analysis. Two patients of the 17 selected did not have quantifiable imaging, one due to post-surgical changes and one because of local structural obfuscation, and these were not included in our cohort [see figure 1].

Figure 1.

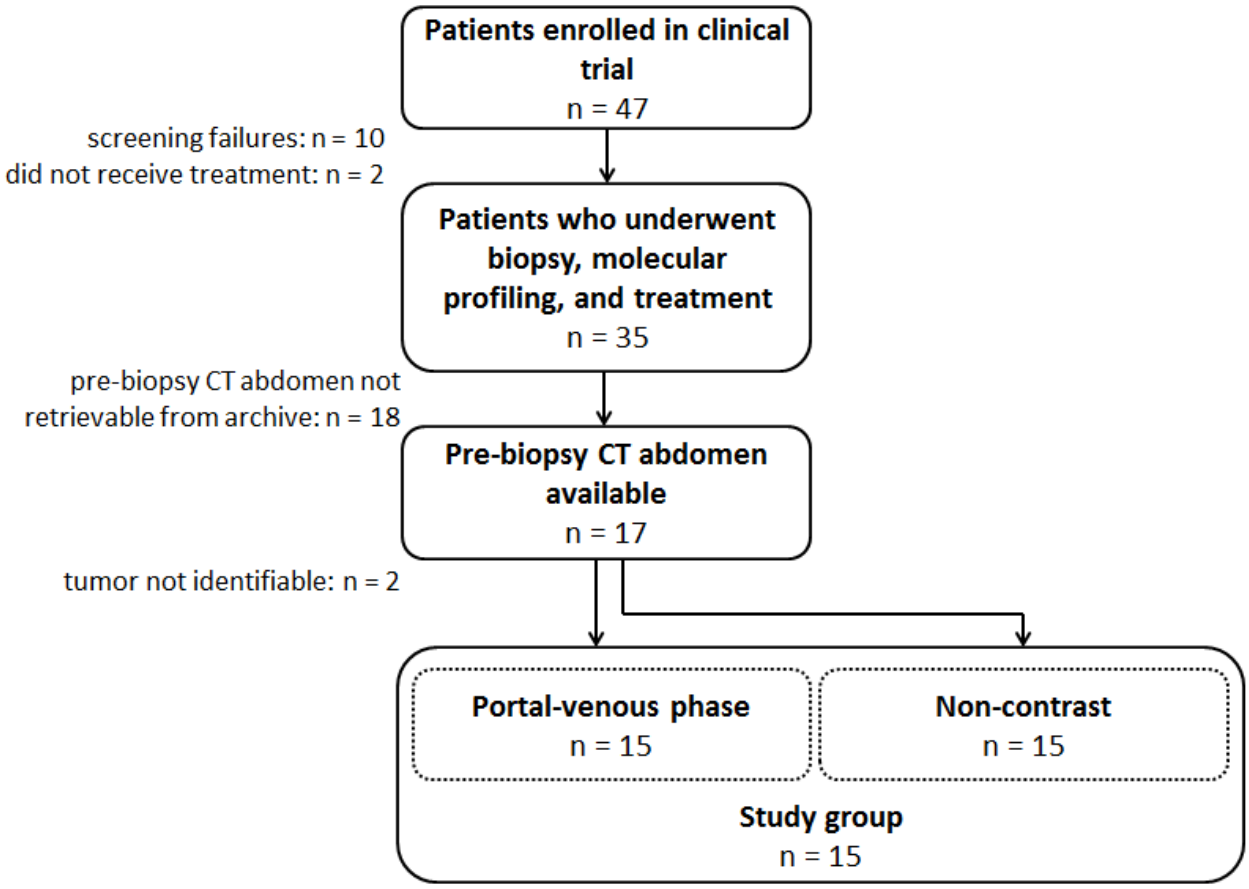
Patients enrolled in clinical trial
n = 47
screening failures: n = 10
did not receive treatment: n = 2
Patients who underwent biopsy, molecular profiling, and treatment
n = 35
pre-biopsy CT abdomen not retrievable from archive: n = 18
Pre-biopsy CT abdomen available
n = 17
tumor not identifiable: n = 2
Portal-venous phase
n = 15
Non-contrast
n = 15
Study group
n = 15

The final cohort included 15 patients. There were 9 men and 6 women. Age ranged from 34 to 71 years old with a median age of 59. CA 19-9 value at the start of treatment, which was available for 11 patients, ranged from 34.2 to 443,796 with a median of 1885.3 [see table 1].

Table 1.

Patient ID	Age	Cancer antigen 19-9 (CA19-9)	Gender	Primary tumor location	Copy number variations (CNV)	Overall survival (OS) in days
4	42	13956	M	head	10	1
5	59	-	F	body	11	190
6	34	12078.5	M	head	52	42
14	70	1885.3	F	head	18	92
22	54	298.6	M	head	13	230
27	64	34.2	M	tail	5	80
32	61	352.1	F	head	12	43
33	67	3063	M	body	22	157
35	56	-	F	body	25	372
36	56	-	M	tail	17	33
38	64	1191	M	head	6	179
42	65	-	F	head	15	120
45	53	539.9	M	head	31	161
48	46	443796	F	head	7	-
49	71	14367	M	head	34	120
median	59	1885.3			15	120

All 15 patients had contrast-enhanced portal venous phase and non-contrast CT scans of the abdomen available. Imaging data were downloaded from the hospital PACS onto a OsiriX™ (Pixmeo, Bernex, Switzerland) DICOM-viewing Mac workstation, de-identified using the unique patient IDs assigned during the clinical trial, and transferred to the TexRAD™ (TexRAD Ltd, Brighton, England) database for analysis. TexRAD is a proprietary software algorithm developed by Ganeshan et al for the analysis of medical images.

CTTA analysis of primary tumor and apparently normal pancreas

For each imaging study, the primary PDAC site and the region of apparently normal pancreas were identified on axial views. An image that contained the most representative section of the tumor and a separate image that best represented the normal pancreas were selected for analysis. These images were loaded into the TexRad software platform. Two regions of interest (ROI) were drawn, the first around the primary tumor and the second around the normal-appearing pancreas. The ROIs were drawn by the medical student and then subsequently reviewed and modified by a board-certified radiologist to independently verify accurate tissue identification.

The initial step in textural analysis is filtering and smoothing of the original image to accentuate macroscopic features and attenuate random photon noise[23]. The TexRad platform utilizes a Laplacian of Gaussian band-pass filter that generates spatial scaling factor (ssf) filter densities of 2, 3, 4, 5, and 6 pixels. Filtering densities were classified as fine (ssf = 2), medium (ssf = 3, 4) and coarse (ssf = 5, 6). One consequence of filtering is that smaller ROIs become unanalyzable at larger filtering densities. As the filter size increases, the boundary edges of the ROI that are not analyzed become larger and encroach upon the analyzed region. This is especially relevant when the tissue has a restricted short axis, such as the oblong shape of the normal pancreas. For this reason, our number of patients was reduced with larger filtering densities when studying the normal pancreas (ssf = 5 with n = 12, ssf = 6 with n = 11) [see figure 2].

Figure 2. Sample of CT textural analysis of PDAC. (**A**) A ROI is drawn around the primary tumor mass in the pancreas. False color texture output shown at fine(**B**), medium (**C)**, and coarse (**D**) filter levels accentuates post-filtering regions. With larger filtering sizes, the boundary edge of the unanalyzable region grows larger (**D, arrows)**. CTTA parameters are calculated for each filter density and recorded into a spreadsheet (not shown).

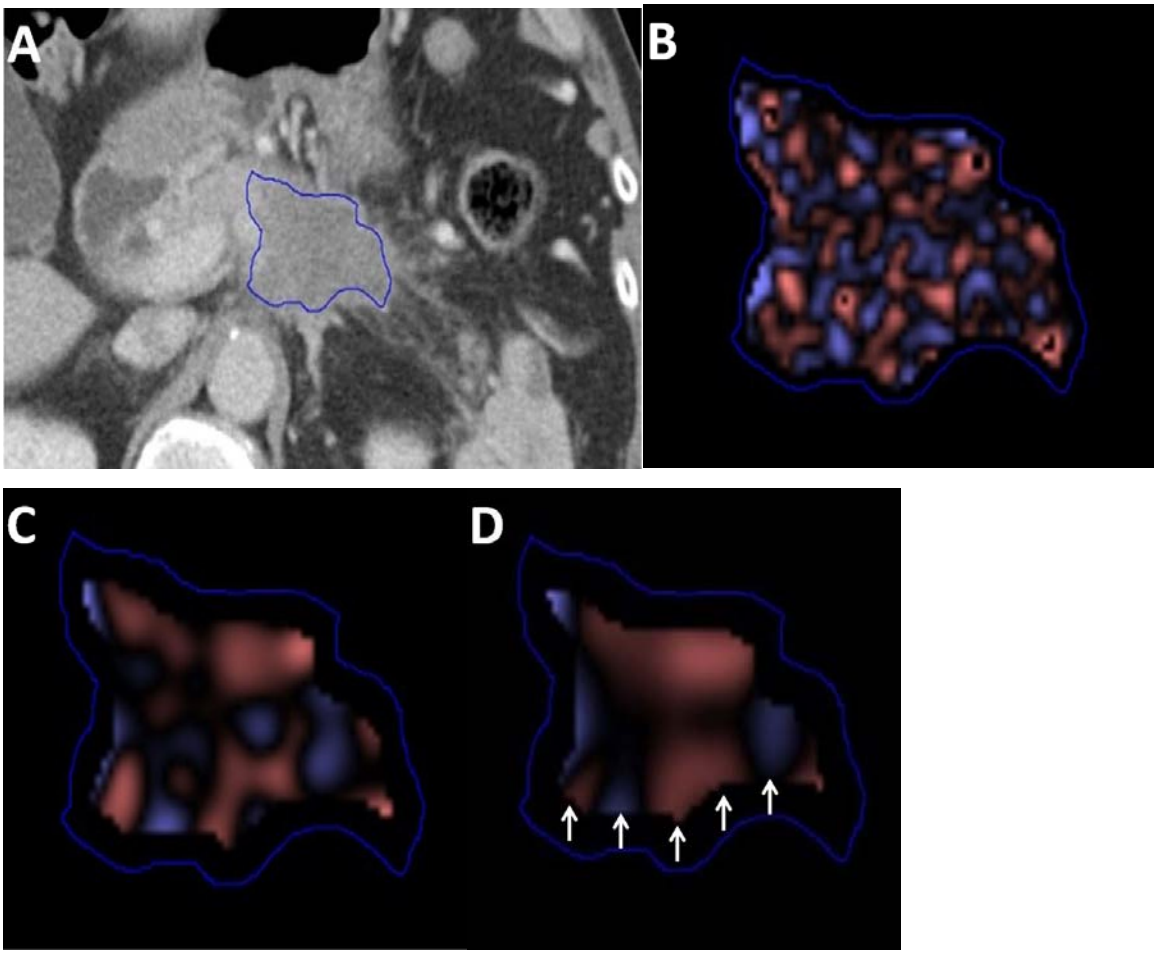

Next, post-filtering individual histograms of pixel data were generated for each ROI at each filtering density. From these histograms, CTTA statistical parameters were generated. These included mean positive pixels (MPP), entropy, kurtosis, and skewness. CTTA parameters were then compared to intrachromosomal CNV per tumor identified by CGH using a Spearman's rank correlation coefficient. In an attempt to normalize tumor to the normal pancreas and assess interplay, we also compared a set of CTTA parameters from the tumor after subtracting the corresponding values from the normal pancreas. After our primary analysis, an exploratory analysis comparing CTTA parameters to overall survival in the cohort was completed using the same methodology. All analyses were separately performed in portal-venous phase and non-contrast image sets.

Results

Copy number variation, overall survival, and CTTA values

Intrachromosomal copy number variations (CNV) were obtained from CGH analysis of metastatic sites for the 15 patients that imaging data were available for. Used in this study as a surrogate for dsDNA breaks and genomic instability, CNV ranged from 5 to 52. Median CNV was 14. Prior experience had revealed that CNV greater than 10 is elevated and consistent with defects in DNA repair. BRCA testing was also completed for the patients on this clinical trial, but none of the patients in our cohort were BRCA positive. Overall survival (OS) was recorded for the 14 out of 15 patients who were deceased at the time of analysis. Median OS was 120 days and ranged from 1 day to 372 days post-treatment.

Primary tumor ROIs, normal pancreas ROIs, and subtracted ROIs were analyzed using TexRAD. CTTA values were generated separately at each filter density (ssf 0, 2, 3, 4, 5, 6), and tabulated results were recorded into a spreadsheet. CTTA values were grouped first by ROI category and then by filtering density. Each parameter was compared to CNV and then to OS using a Spearman's rank correlation [see table 2].

Comparison of copy number variation to CT texture analysis

A statistically significant correlation with CNV was observed using kurtosis of the primary tumor mass. CNV were negatively correlated with kurtosis (median: -0.146; range: -0.810 to 0.633) using medium texture filtering ($p = 0.034$, $n = 15$; ssf = 3). A linear regression established that kurtosis of the primary tumor at medium texture filtering (ssf = 3) statistically significantly predicts CNV ($t = -2.311$, $p = 0.038$). The regression equation was: predicted CNV = 16.964 – [16.041 x (kurtosis)] [figure 3]. The remaining CTTA values of entropy, skewness, and mean positive pixels were not significant at this filtering density. Medium filtering (ssf = 3) analysis of the normal pancreas ROIs and subtracted ROIs were also non-significant.

Figure 3. Linear regression plot of CNV vs. kurtosis of the primary tumor at medium texture filtering (p = 0.038, n = 15, ssf = 3)

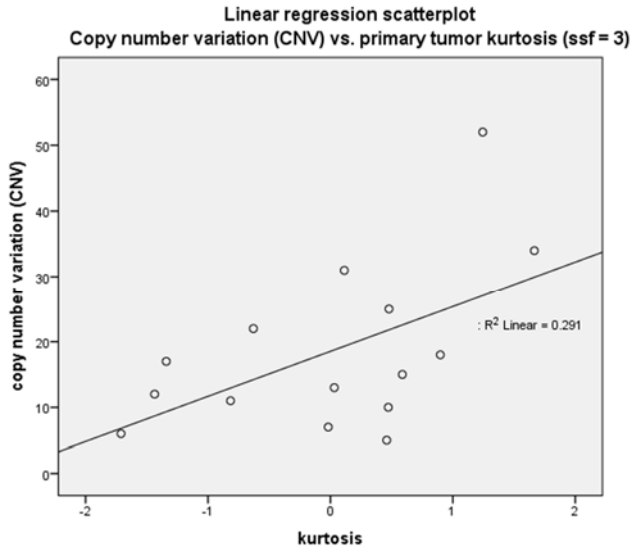

Analysis of copy number variations (CNV) compared to the CTTA values of the tumor ROIs, normal pancreas ROIs, and subtracted ROIs at all other filtering densities (ssf = 0, 2, 4, 5, 6) revealed no additional significant correlations using a Spearman's rank correlation coefficient (see table 2).

Table 2. Summary of Spearman's rank correlations with significant results highlighted.

	ssf			entropy	mpp	skewness	kurtosis
Tumor ROIs	0	CNV	Correlation Coefficient	.304	-.021	.136	-.246
			Sig. (2-tailed)	.271	.940	.630	.376
			N	15	15	15	15
		OS	Correlation Coefficient	-.167	-.077	.372	-.392
			Sig. (2-tailed)	.568	.794	.190	.166
			N	14	14	14	14
	2	CNV	Correlation Coefficient	.143	.171	-.004	-.018
			Sig. (2-tailed)	.612	.541	.990	.950
			N	15	15	15	15
		OS	Correlation Coefficient	-.051	-.178	-.163	.370
			Sig. (2-tailed)	.864	.542	.578	.193
			N	14	14	14	14
	3	CNV	Correlation Coefficient	.175	.050	.039	**-.550***
			Sig. (2-tailed)	.533	.860	.889	**.034**
			N	15	15	15	**15**
		OS	Correlation Coefficient	.218	-.026	-.493	.150
			Sig. (2-tailed)	.454	.929	.073	.610
			N	14	14	14	14
	4	CNV	Correlation Coefficient	.082	-.171	-.018	-.461
			Sig. (2-tailed)	.771	.541	.950	.084
			N	15	15	15	15
		OS	Correlation Coefficient	.191	.059	-.189	.238
			Sig. (2-tailed)	.512	.840	.517	.413
			N	14	14	14	14
	5	CNV	Correlation Coefficient	-.107	-.143	-.096	-.371
			Sig. (2-tailed)	.704	.612	.732	.173
			N	15	15	15	15
		OS	Correlation Coefficient	.121	-.026	-.394	.517
			Sig. (2-tailed)	.680	.929	.164	.058
			N	14	14	14	14
	6	CNV	Correlation Coefficient	-.043	-.271	.164	-.418
			Sig. (2-tailed)	.879	.328	.558	.121
			N	15	15	15	15
		OS	Correlation Coefficient	.075	-.176	-.037	.273
			Sig. (2-tailed)	.799	.547	.899	.345
			N	14	14	14	14

	ssf			entropy	mpp	skewness	kurtosis
Normal pancreas ROIs	0	CNV	Correlation Coefficient	.033	.200	.235	-.160
			Sig. (2-tailed)	.911	.493	.418	.584
			N	14	14	14	14
		OS	Correlation Coefficient	-.211	-.207	.136	.130
			Sig. (2-tailed)	.469	.478	.642	.658
			N	14	14	14	14
	2	CNV	Correlation Coefficient	.007	.152	-.002	-.152
			Sig. (2-tailed)	.982	.605	.994	.605
			N	14	14	14	14
		OS	Correlation Coefficient	-.306	-.125	-.079	.205
			Sig. (2-tailed)	.288	.669	.788	.483
			N	14	14	14	14
	3	CNV	Correlation Coefficient	-.024	.116	-.029	-.226
			Sig. (2-tailed)	.935	.692	.923	.436
			N	14	14	14	14
		OS	Correlation Coefficient	-.422	-.015	-.011	.218
			Sig. (2-tailed)	.132	.958	.970	.454
			N	14	14	14	14
	4	CNV	Correlation Coefficient	-.081	.301	-.064	-.248
			Sig. (2-tailed)	.782	.296	.829	.392
			N	14	14	14	14
		OS	Correlation Coefficient	-.471	-.154	.031	.271
			Sig. (2-tailed)	.089	.599	.917	.349
			N	14	14	14	14
	5	CNV	Correlation Coefficient	.126	.196	.119	-.252
			Sig. (2-tailed)	.697	.542	.713	.430
			N	12	12	12	12
		OS	Correlation Coefficient	**-.809****	-.312	.186	-.235
			Sig. (2-tailed)	**.001**	.324	.564	.463
			N	**12**	12	12	12
	6	CNV	Correlation Coefficient	-.282	.309	.264	.145
			Sig. (2-tailed)	.401	.355	.433	.670
			N	11	11	11	11
		OS	Correlation Coefficient	-.574	-.023	.246	-.023
			Sig. (2-tailed)	.065	.947	.466	.947
			N	11	11	11	11

	ssf			entropy	mpp	skewness	kurtosis
Subtraction ROIs	0	CNV	Correlation Coefficient	.279	-.296	-.239	.064
			Sig. (2-tailed)	.315	.283	.390	.820
			N	15	15	15	15
		OS	Correlation Coefficient	.248	-.036	.005	-.252
			Sig. (2-tailed)	.372	.899	.985	.365
			N	15	15	15	15
	2	CNV	Correlation Coefficient	.257	-.039	.139	.111
			Sig. (2-tailed)	.355	.889	.621	.694
			N	15	15	15	15
		OS	Correlation Coefficient	.218	.107	.236	.181
			Sig. (2-tailed)	.435	.704	.397	.520
			N	15	15	15	15
	3	CNV	Correlation Coefficient	.254	-.154	.121	-.029
			Sig. (2-tailed)	.362	.585	.666	.919
			N	15	15	15	15
		OS	Correlation Coefficient	.265	.343	.013	-.068
			Sig. (2-tailed)	.341	.210	.965	.810
			N	15	15	15	15
	4	CNV	Correlation Coefficient	.279	-.300	.143	.018
			Sig. (2-tailed)	.315	.277	.612	.950
			N	15	15	15	15
		OS	Correlation Coefficient	.418	.175	.145	.046
			Sig. (2-tailed)	.121	.532	.607	.869
			N	15	15	15	15
	5	CNV	Correlation Coefficient	-.035	-.224	-.224	-.091
			Sig. (2-tailed)	.914	.484	.484	.779
			N	12	12	12	12
		OS	Correlation Coefficient	.529	.088	-.294	.263
			Sig. (2-tailed)	.077	.787	.353	.409
			N	12	12	12	12
	6	CNV	Correlation Coefficient	.077	-.168	-.168	-.308
			Sig. (2-tailed)	.812	.602	.602	.331
			N	12	12	12	12
		OS	Correlation Coefficient	.350	-.025	.224	.105
			Sig. (2-tailed)	.264	.940	.484	.745
			N	12	12	12	12

A multiple linear regression was performed to predict CNV from CTTA values (mean positive pixels, entropy, kurtosis, skewness), but this did not reveal any statistically significant predictive correlation (data not shown).

Comparison of overall survival to CT texture analysis

Secondary analysis of the normal pancreas was performed in a similar fashion to assess if any CTTA parameters were predictive of overall survival (OS) in the cohort. All parameters derived from the tumor ROIs, normal pancreas ROIs, and subtracted ROIs were compared to OS using a Spearman's rank correlation. Kurtosis, skewness, and mean positive pixels showed no significant relationship at all filter densities.

Entropy of the normal pancreas using coarse texture filtering (ssf = 5) did yield a significant correlation with OS. Increasing entropy was strongly correlated with decreased OS using a Spearman's rank correlation ($p = 0.0014$, $n = 12$; ssf = 5). Linear regression analysis failed to establish a statistically significant linear relationship between entropy and OS ($p = 0.057$) [figure 4]. However, given that the Spearman correlation was strong, an attempt was made to categorize high entropy versus low entropy to elicit a difference between the two groups. Using median entropy as a cutoff value (median: 4.165; range 2.686 – 4.891), median OS was greater in the entropy < 4.165 group versus the entropy > 4.165 group (179 days v 43 days, respectively; 95% CI 73.137 – 166.87; $p = 0.004$, $n = 12$) [figure 5].

Figure 4. Linear regression plot of OS vs. kurtosis of the normal pancreas at coarse texture filtering (ns, n = 12, ssf = 5)

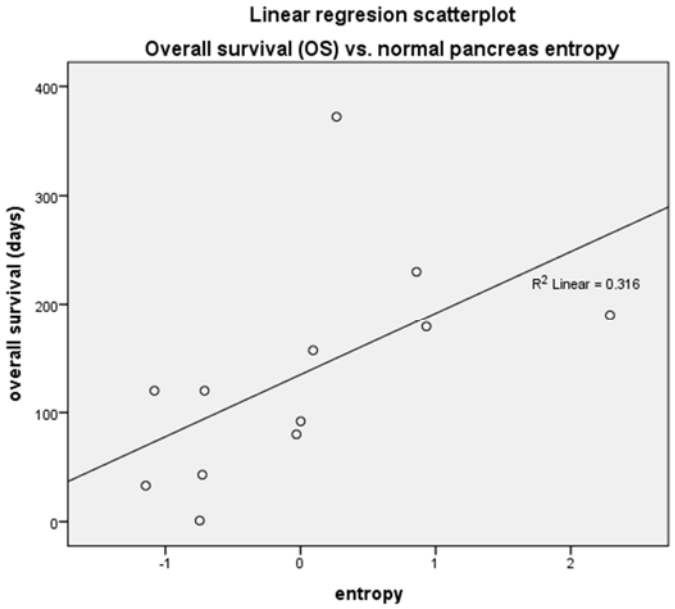

Figure 5. Kaplan-Meier plot of OS at high entropy (> 4.165) and low entropy (<4.165) values of the normal pancreas with coarse texture filtering (ssf = 5)

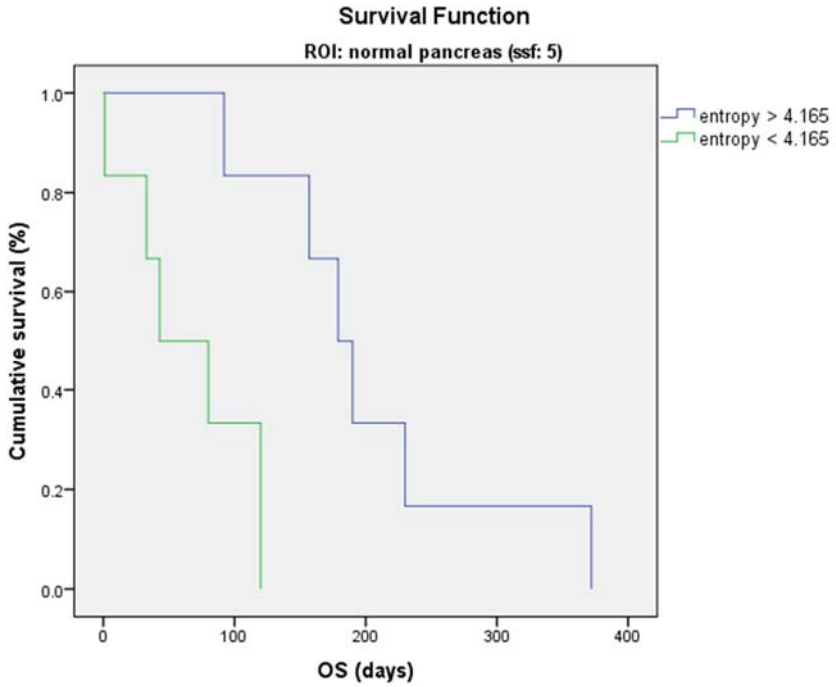

A multiple linear regression was performed to predict OS from CTTA values (mean positive pixels, entropy, kurtosis, skewness), which did not reveal any statistically significant predictive correlation (data not shown).

Discussion

In this pilot study of metastatic, treatment-resistant pancreatic ductal adenocarcinoma (PDAC), we sought to apply CT textural analysis (CTTA) to primary tumors and the apparently normal pancreas to determine if tumors with deficits in DNA repair, represented by increased copy number variation (CNV), could be identified with the technique. We found that kurtosis of the primary tumor mass using medium filtering was correlated with CNV in metastatic sites ($p = 0.034$, $n = 15$, ssf = 3). Secondarily, we investigated the QTTA features for a prognostic association to overall survival (OS). Increasing entropy in the normal pancreas, a measure of the tissue heterogeneity, was associated with decreased OS using coarse texture filtering ($p = 0.0014$, $n = 12$, ssf = 5). These results support the use of CTTA to assess genetic abnormalities and prognosis in PDAC.

PDAC and the tumor microenvironment

The current understanding of carcinogenesis has expanded to appreciate the heterogeneity of the tumor microenvironment. It has become apparent that the interaction between cancer cells and the surrounding stroma generate an interplay dependent on access to nutrients and oxygen, driving pluripotent cancer cells to develop adaptive mutations that enhance survival in their individual milieu. This evolution selects for oncogenetic pathways that sustain survival and proliferation and repress mechanisms for exiting the cell cycle[24]. Consistent with the transition of neoplasia to malignancy, invasion, and eventual metastasis is the inactivation or bypass of tumor suppressor genes. Control of the cell cycle through P16/CDKN2A is critically disrupted in 95% of PDACs via homozygous deletion, loss of allele mutation, or silencing. SMAD and p53 are also frequently reported loss of function mutations. SMAD4 inactivation in particular is associated with increased metastatic burden and decreased survival[25].

PDAC also harbors an unusual preference for glucose uptake, aerobic glycolysis, and lactic acid fermentation. Functionally, this allows it to exist and thrive in a hypoxic environment. This process of glycolytic hypermetabolism is tied to oncogenically transformed components of the K-Ras pathway, an activating mutation in greater than 90% of PDACs. In addition, the dense stroma and poor vasculature exposes tumor cells to hypoxia, which triggers Ras-augmented HIF-1α dependent autophagy, a key pathway for pancreatic cancer cell survival. Lactic acid, the

end-product of glycolysis in hypoxic conditions also acts in an immunosuppressive manner by accumulating and impairing T-cell metabolism and function. What results is an environmentally-attuned malignant cell line that elusively evades the immune system by generating immunosuppressive metabolic bi-products and insulates itself from chemotherapeutics by generating a dense extracellular matrix and restricted vascular supply[24].

The heterogeneous, slightly hypodense, disordered appearance on contrast-enhanced CT scan of malignant PDAC is the result of this poorly vascularized, hypoxic stroma[26,27]. As much as 80% of the primary tumor mass consists of fibrotic tissue produced by activated fibroblasts and pancreatic stellate cells[26]. Chronic inflammation stimulates and supports this desmoplastic response, enhancing carcinogenic processes and protecting tumorogenic cells from chemotherapeutic delivery[28]. It is interesting to note that in animal studies, development of PanIN or PDAC in oncogenically transformed KRAS cells is dependent upon the setting of chronic pancreatitis, suggesting that inflammation is actually a prerequisite to carcinogenesis[27]. The 50 to 80-fold increased risk for PDAC in patients with hereditary pancreatitis would support this theory, though studies have not supported chronic pancreatitis to be an isolated inciting event for PDAC[2].

These genetic and phenotypic features, some unique to PDAC and others common to many other solid cancers, define the environment of the primary tumor and founder genomes of its metastatic progeny. A multitude of approaches for screening and early detection are being explored to detect PDAC prior to its lethal systemic dissemination[29], but currently the clinical focus remains on improving survival in patients with metastatic disease.

CT imaging of pancreatic ductal adenocarcinoma

CT imaging with contrast enhancement has been established as the standard-of-care for imaging suspected pancreatic malignancy, staging, and much of follow-up. The most common location of primary tumors is in the head of the pancreas. Triple phase contrast-enhanced multi-detector CT has an 86 – 97% sensitivity for detection, but this drops to 77% for tumors less than 2 cm[30]. High-grade PanIN-3 lesions are recognized as carcinoma *in situ*, though their miniscule size prevents detection on CT[26]**.** Other imaging modalities such as EUS and MRI have also shown additional efficacy in certain clinical scenarios, particularly in evaluating tumors less

than 3 cm and assessing the degree of vascular invasion, respectively. However, contrast-enhanced CT has been demonstrated to either equal or supersede the accuracy of these modalities overall[31]. PET CT has been studied as well, showing no advantage over contrast-enhanced CT[32]. Widely available, equal in accuracy to MRI/MRCP, and serially performed, the ubiquity of contrast-enhanced CT for imaging PDAC renders it particularly exploitable in terms of further analysis.

CT textural analysis parameters as biomarkers

CT textural analysis (CTTA) is a promising clinical tool that interrogates an ROI, filters out noise, translates the distribution of gray-level intensities into a histogram, and generates numerical statistical parameters based on the histogram. It has been shown that these CTTA parameters are exploitable in terms of analysis because of their dependence upon architectural characteristics of the underlying tissue such as heterogeneity and vascularity[33].

Given that the tumor and its associated stroma is a direct result of gene expression in response to a particular environment, it is plausible to correlate imaging features to genetics. Computerized textural analysis of medical imaging is not a new idea[34], but the advent of widely available, transferable imaging through PACS, clinical availability of detailed genomic data, and improved software platforms has led to a resurgence of investigating the application of textural analysis to cancer. The use of CTTA parameters as biomarkers has been studied in colorectal cancer, squamous cell cancer of the head and neck, cerebral gliomas, hepatocellular carcinoma, non-squamous cell lung cancer, esophageal cancer, lymphoma, and renal cell carcinoma. Correlations with relevant histopathologic features such as tumoral vascularity, grading and staging, gene amplification, and differentiating malignant versus benign lesions have been revealed[4-10,14,35]. Additionally, relevant clinical endpoints like overall survival and treatment response have also been correlated with CTTA features[11-17]. However, no CTTA studies on pancreatic ductal adenocarcinoma (PDAC) are currently published in the literature.

In this study, we investigated the novel application of CTTA to metastatic, treatment-resistant PDAC. This is a hardened disease entity that has survived and evolved in response to cytotoxic and antimetabolite chemotherapeutics. Given this challenging presentation, harvesting clues of the tumor genome and environment from imaging would augment the

clinician's ability to evaluate treatment response and gauge prognosis. By analyzing primary tumor lesions and the apparently unaffected pancreas, we showed that CTTA parameters extracted from routinely acquired CT imaging can correlate to treatment-relevant genomic and prognostic features.

Kurtotis and copy number variation

Specifically, intrachromosomal copy number variations (CNV) of metastatic biopsy sites, a marker for impaired DNA repair and unstable tumor genetics, were correlated negatively with kurtosis of the primary tumor using medium-texture filtering ($p = 0.034$, $n = 15$; ssf = 3). Kurtosis is a measure of the "peakedness" of the gray-level intensity histogram. A more negative kurtosis is therefore associated with a flatter distribution of pixels compared to a normal Gaussian distribution. Regions of low to negative kurtosis are consistent with a larger distribution of tissue types. This heterogeneity could be in part due to impaired DNA repair. Negative kurtosis has been shown to correlate with decreased overall survival in CRC[12]. It is not clear why this particular parameter negatively correlated with dsDNA breaks, but it is possible that the process itself or the environment it exists in lends itself to detection by CTTA kurtosis. Further studies would be required to elucidate the relationship.

Entropy and overall survival

Our secondary exploration of CTTA parameters in regard to clinical outcomes also yielded an interesting association. Increased entropy in the apparently disease-free region of the pancreas was correlated with decreased overall survival ($p = 0.0014$, ssf = 5). Additionally, analysis of the filter settings below and above this also approached significance ($p = 0.089$, ssf = 4; $p = 0.065$, ssf = 6). While exploratory in nature, this is very intriguing because it concurs with previously published findings in other cancers. A CTTA investigation of apparently disease-free areas of the liver in the setting of metastatic colorectal cancer showed that increasing entropy was associated with radiographically occult liver metastases[36]. Other studies showed that CTTA parameters of CRC metastatic lesions are prognostic in CRC, and entropy in particular was strongly associated with decreased overall survival[10,12,37]. It is possible that an underlying inflammatory process, such as a radiographically occult pancreatitis or tumor invasion, is

disrupting the apparently normal pancreatic tissue. Whatever the case, the disruption in the architecture is detectable with CTTA, and it is prognostically poor.

Limitations

The primary limitation in this study was a small sample size. Of the original 35 patients who completed the clinical trial, only 15 patients had analyzable venous phase and non-contrast CTs available in the imaging database. There was also incomplete clinical information from the trial with respect to individual patient characteristics. An overall summary of previous treatment regimens, tumor metastatic sites, and demographic characteristics was included in the clinical trial data, but there was no breakdown for individual patients. Since the imaging database only had data for a limited number of patients, these summary patient characteristics could not be applied to our study to control confounding variables that may have been present.

CNV by array CGH is a very useful method for detecting unbalanced chromosomal aberrations in the form of amplifications or deletions. However, it must be noted that the technique does not detect other forms of structural variation such as reciprocal translocations, inversions, and ring chromosomes[22]. Additionally, our CTTA analysis of the primary tumor was compared to CGH results from biopsied metastatic sites, which were variable. Studies in colorectal cancer have shown that though primary tumor populations and metastatic sites are not identical, they share the same large scale genetic features[38]. Therefore we can surmise that PDAC metastatic sites should share similar enough genetics to the primary tumor, but biopsy specimens from the primary tumor would be a more direct comparison.

Another caveat is the exploratory nature of the study. As CTTA has never been applied to PDAC, there were no previous studies to measure our results against. While CTTA has been studied in other cancers, it would be wrong to assume that these associations would yield the same result in PDAC. Therefore we explored multiple CTTA parameters at all available filtering densities. And while it was interesting that entropy seemed to exhibit a strong signal on its correlation with overall survival, it was not part of our original hypothesis.

Future directions

These two intriguing correlations with genomic and prognostic features is proof of concept that CTTA can be successfully applied to metastatic PDAC. At minimal cost with no additional imaging, biopsy, or molecular profiling, textural analysis of standard-of-care routine CT imaging can be used to harvest additional, actionable information for patients with this disease.

If validated with a larger sample set, the results of CTTA would be of value in selecting DNA-damaging treatment regimens with patients whose primary tumor exhibits low kurtosis. Platinum-containing cytotoxic regimens, shown to be of benefit, could be implemented sooner. This would be of special value in resource-poor settings where biopsy with molecular profiling is not readily available. Textural analysis is very feasible and easy to implement, and this clinical information to guide treatment would be beneficial.

Overall survival and normal pancreatic entropy is perhaps the most interesting association revealed. While also requiring a larger sample set for validation and further study, it would be much more feasible to implement than studying dsDNA breaks versus tumor kurtosis. Molecular profiling data would not be required. All that would be need for each patient is a non-contrast CT abdomen scan, overall survival since the scan, and patient characteristics. Unfortunately, the Cancer Imaging Archive does not yet contain imaging for PDAC, so the imaging data would need to be pooled from an institution that commonly treats the disease.

Conclusions

This novel exploration of CTTA and PDAC revealed intriguing associations between imaging, tumor genetics, and prognosis. Though still a relatively uncommon cancer, PDAC's lethality and aggressiveness render its impact disproportionally severe. Given the lack of suitable tests to guide treatment at the metastatic stage, textural analysis of existing CT imaging could become a helpful tool in the limited arsenal against a robust and very malignant disease. Much more research is needed to validate the usefulness of these associations. With increasing connectivity between PACS platforms and growing cancer imaging archives, the practicality of applying textural analysis to rarer cancer entities like PDAC is more feasible than ever. We assert that this study is proof of concept that CT textural analysis can be successfully applied to PDAC.

References

1. Porta M, Fabregat X, Malats N, et al. Exocrine pancreatic cancer: Symptoms at presentation and their relation to tumour site and stage. *Clinical and Translational Oncology*. 2005;7(5):189-197.

2. Yeo TP. Demographics, epidemiology, and inheritance of pancreatic ductal adenocarcinoma. . 2015;42(1):8-18.

3. O'Reilly EM, Lowery MA, Segal MF, et al. Phase IB trial of cisplatin (C), gemcitabine (G), and veliparib (V) in patients with known or potential BRCA or PALB2-mutated pancreas adenocarcinoma (PC). . 2014;32(15_suppl):4023.

4. Hayano K, Tian F, Kambadakone AR, et al. Texture analysis of non-contrast-enhanced computed tomography for assessing angiogenesis and survival of soft tissue sarcoma. *J Comput Assist Tomogr*. 2015.

5. Hodgdon T, McInnes MD, Schieda N, Flood TA, Lamb L, Thornhill RE. Can quantitative CT texture analysis be used to differentiate fat-poor renal angiomyolipoma from renal cell carcinoma on unenhanced CT images? *Radiology*. 2015:142215.

6. Skogen K, Ganeshan B, Good C, Critchley G, Miles K. Measurements of heterogeneity in gliomas on computed tomography relationship to tumour grade. *J Neurooncol*. 2013;111(2):213-219.

7. Ganeshan B, Abaleke S, Young RC, Chatwin CR, Miles KA. Texture analysis of non-small cell lung cancer on unenhanced computed tomography: Initial evidence for a relationship with tumour glucose metabolism and stage. *Cancer Imaging*. 2010;10:137-143.

8. Weiss GJ, Ganeshan B, Miles KA, et al. Noninvasive image texture analysis differentiates K-ras mutation from pan-wildtype NSCLC and is prognostic. . 2014.

9. Ganeshan B, Goh V, Mandeville HC, Ng QS, Hoskin PJ, Miles KA. Non–small cell lung cancer: Histopathologic correlates for texture parameters at CT. *Radiology*. 2013;266(1):326-336.

10. Ganeshan B, Miles KA, Young RC, Chatwin CR. Hepatic enhancement in colorectal cancer: Texture analysis correlates with hepatic hemodynamics and patient survival. *Acad Radiol*. 2007;14(12):1520-1530.

11. Ganeshan B, Panayiotou E, Burnand K, Dizdarevic S, Miles K. Tumour heterogeneity in non-small cell lung carcinoma assessed by CT texture analysis: A potential marker of survival. *Eur Radiol*. 2012;22(4):796-802.
12. Ng F, Ganeshan B, Kozarski R, Miles KA, Goh V. Assessment of primary colorectal cancer heterogeneity by using whole-tumor texture analysis: Contrast-enhanced CT texture as a biomarker of 5-year survival. *Radiology*. 2013;266(1):177-184.
13. Zhang H, Graham CM, Elci O, et al. Locally advanced squamous cell carcinoma of the head and neck: CT texture and histogram analysis allow independent prediction of overall survival in patients treated with induction chemotherapy. *Radiology*. 2013;269(3):801-809.
14. Ganeshan B, Skogen K, Pressney I, Coutroubis D, Miles K. Tumour heterogeneity in oesophageal cancer assessed by CT texture analysis: Preliminary evidence of an association with tumour metabolism, stage, and survival. *Clin Radiol*. 2012;67(2):157-164.
15. Abel EJ, Lubner M, Munoz Del Rio A, Stabo N, Pickhardt P. Pd4-08 pre-treatment ct textural analysis of large primary renal cell carcinomas; tumor heterogeneity correlates with histology and clinical outcomes. *J Urol*. 2015;193(4):e89-e90.
16. Ganeshan B, Miles K, Babikir S, Shortman R, Groves A, Kayani I. Low dose CT texture analysis (CTTA) can potentially sub-classify risk in lymphoma patients showing complete metabolic response on interim PET. *Journal of Nuclear Medicine*. 2014;55(supplement 1):452-452.
17. Goh V, Ganeshan B, Nathan P, Juttla JK, Vinayan A, Miles KA. Assessment of response to tyrosine kinase inhibitors in metastatic renal cell cancer: CT texture as a predictive biomarker. *Radiology*. 2011;261(1):165-171.
18. Waddell N, Pajic M, Patch A, et al. Whole genomes redefine the mutational landscape of pancreatic cancer. *Nature*. 2015;518(7540):495-501.
19. Golan T, Kanji Z, Epelbaum R, et al. Overall survival and clinical characteristics of pancreatic cancer in BRCA mutation carriers. *Br J Cancer*. 2014;111(6):1132-1138.
20. Barrett MT, Lenkiewicz E, Evers L, et al. Phase II study of therapy selected by molecular profiling in patients with previously treated metastatic pancreatic cancer-SU2C-001. *Cancer Res*. 2012;72(8 Supplement):3697-3697.

21. Bejjani BA, Shaffer LG. Application of array-based comparative genomic hybridization to clinical diagnostics. *The Journal of Molecular Diagnostics*. 2006;8(5):528-533.
22. Weiss MM, Hermsen MA, Meijer GA, et al. Comparative genomic hybridisation. *Mol Pathol*. 1999;52(5):243-251.
23. Miles KA, Ganeshan B, Hayball MP. CT texture analysis using the filtration-histogram method: What do the measurements mean? *Cancer Imaging*. 2013;13(3):400-406.
24. Blum R, Kloog Y. Metabolism addiction in pancreatic cancer. *Cell death & disease*. 2014;5(2):e1065.
25. Ryan DP, Hong TS, Bardeesy N. Pancreatic adenocarcinoma. *N Engl J Med*. 2014;371(22):2139-2141.
26. Erkan M, Hausmann S, Michalski CW, et al. The role of stroma in pancreatic cancer: Diagnostic and therapeutic implications. *Nature Reviews Gastroenterology and Hepatology*. 2012;9(8):454-467.
27. Guturu P, Shah V, Urrutia R. Interplay of tumor microenvironment cell types with parenchymal cells in pancreatic cancer development and therapeutic implications. *Journal of gastrointestinal cancer*. 2009;40(1-2):1-9.
28. Erkan M, Reiser-Erkan C, W Michalski C, et al. The impact of the activated stroma on pancreatic ductal adenocarcinoma biology and therapy resistance. *Curr Mol Med*. 2012;12(3):288-303.
29. Lennon AM, Wolfgang CL, Canto MI, et al. The early detection of pancreatic cancer: What will it take to diagnose and treat curable pancreatic neoplasia? *Cancer Res*. 2014;74(13):3381-3389.
30. Bronstein YL, Loyer EM, Kaur H, et al. Detection of small pancreatic tumors with multiphasic helical CT. *Am J Roentgenol*. 2004;182(3):619-623.
31. Tamm EP, Bhosale PR, Lee JH. Pancreatic ductal adenocarcinoma: Ultrasound, computed tomography, and magnetic resonance imaging features. *Seminars in Ultrasound, CT and MRI*. 2007;28(5):330-338.

32. Rijkers A, Valkema R, Duivenvoorden H, van Eijck C. Usefulness of F-18-fluorodeoxyglucose positron emission tomography to confirm suspected pancreatic cancer: A meta-analysis. *European Journal of Surgical Oncology (EJSO)*. 2014;40(7):794-804.
33. Ganeshan B, Miles KA. Quantifying tumour heterogeneity with CT. *Cancer Imaging*. 2013;13:140-149.
34. Tully RJ, Conners RW, Harlow CA, Lodwick GS. Towards computer analysis of pulmonary infiltration. *Invest Radiol*. 1978;13(4):298-305.
35. Kuo MD, Gollub J, Sirlin CB, Ooi C, Chen X. Radiogenomic analysis to identify imaging phenotypes associated with drug response gene expression programs in hepatocellular carcinoma. *Journal of Vascular and Interventional Radiology*. 2007;18(7):821-830.
36. Ganeshan B, Miles KA, Young RC, Chatwin CR. Texture analysis in non-contrast enhanced CT: Impact of malignancy on texture in apparently disease-free areas of the liver. *Eur J Radiol*. 2009;70(1):101-110.
37. Lubner MG, Stabo N, Lubner SJ, et al. CT textural analysis of hepatic metastatic colorectal cancer: Pre-treatment tumor heterogeneity correlates with pathology and clinical outcomes. *Abdom Imaging*. 2015:1-7.
38. Sylvester BE, Vakiani E. Tumor evolution and intratumor heterogeneity in colorectal carcinoma: Insights from comparative genomic profiling of primary tumors and matched metastases. *J Gastrointest Oncol*. 2015;6(6):668-675.

Table 3. Summary of significant findings.

CTTA of primary tumor versus copy number variation (CNV)

(Spearman's rank correlation)

ssf			entropy	mpp	skewness	kurtosis
3	copy number variation (CNV)	Correlation Coefficient	0.1750	0.0500	0.0393	**-0.5500***
		Sig. (2-tailed)	0.5327	0.8595	0.8894	**0.0337**
		N	15	15	15	**15**

CTTA of normal pancreas vs. overall survival (OS)

(Spearman's rank correlation)

ssf			entropy	mpp	skewness	kurtosis
5	overall survival (OS)	Correlation Coefficient	**-0.8091****	-0.3117	0.1856	-0.2347
		Sig. (2-tailed)	**0.0014**	0.3239	0.5635	0.4628
		N	**12**	12	12	12